Potassium-dependent Volume Regulation in Retinal Pigment Epithelium Is Mediated by Na,K,Cl Cotransport

JOSEPH S. ADORANTE and SHELDON S. MILLER

From the School of Optometry and Department of Molecular and Cell Biology, University of California, Berkeley, California 94720

ABSTRACT Changes in retinal pigment epithelial (RPE) cell volume were measured by monitoring changes in intracellular tetramethylammonium (TMA) using double-barreled K-resin microelectrodes. Hyperosmotic addition of 25 or 50 mM mannitol to the Ringer of the apical bath resulted in a rapid (~30 s) osmometric cell shrinkage. The initial cell shrinkage was followed by a much slower (minutes) secondary shrinkage that is probably due to loss of cell solute. When apical $[K^+]$ was elevated from 2 to 5 mM during or before a hyperosmotic pulse, the RPE cell regulated its volume by reswelling towards control within 3–10 min. This change in apical $[K^+]$ is very similar to the increase in subretinal $[K^+]_o$ that occurs after a transition from light to dark in the intact vertebrate eye. The K-dependent regulatory volume increase (RVI) was inhibited by apical Na removal, Cl reduction, or the presence of bumetanide. These results strongly suggest that a Na(K),Cl cotransport mechanism at the apical membrane mediates RVI in the bullfrog RPE. A unique aspect of this cotransporter is that it also functions at a lower rate under steady-state conditions. The transport requirements for Na, K, and Cl, the inhibition of RVI by bumetanide, and thermodynamic calculations indicate that this mechanism transports Na, K, and Cl in the ratio of 1:1:2.

INTRODUCTION

The retinal pigment epithelium (RPE) separates the neural retina from its choroidal blood supply. This single layer of cells is unique in the sense that it functions as a transport epithelium, a macrophage, and a glial cell (Steinberg, 1988). There are a variety of interactions between the RPE and photoreceptors that occur during a transition from the light to dark. These include vitamin A transport and storage, phagocytosis, and epithelial ion and fluid transport (Miller and Steinberg, 1977*a*, *b*; Hughes et al., 1984, 1987; Miller and Farber, 1984; Bok, 1985; Besharse et al., 1987).

Active ion transport-mediated fluid movement across the RPE between the photoreceptors and the choroidal blood supply helps to determine the chemical

Address reprint requests to Dr. Sheldon Miller, 360 Minor Hall, University of California, Berkeley, CA 94720.

J. GEN. PHYSIOL. © The Rockefeller University Press · 0022-1295/90/12/1153/24 $2.00 1153
Volume 96 December 1990 1153–1176

composition of the subretinal space. In addition, the relative hydration state of the subretinal space may be an important determinant of RPE–retina adhesivity (Hughes et al., 1984, 1987; Miller and Farber, 1984; Bird, 1989; Marmor, 1989; Pederson, 1989).

A number of cell types including epithelia are capable of compensating for or preventing changes in cell volume (Eveloff and Warnock, 1987; Larson and Spring, 1987; Hoffman and Simonsen, 1989). In general, osmotic swelling or shrinkage activates net solute flux mechanisms, thereby causing osmotically obliged water to leave or enter the cell, respectively. The return of cell volume toward control level after osmotic swelling or shrinkage has been designated regulatory volume decrease (RVD) or regulatory volume increase (RVI), respectively (Cala, 1980).

In this article we focus on RPE hyperosmotic cell shrinkage and specify the mechanism that returns the cell to control level. For RVI to occur, apical K^+ must be elevated from 2 to 5 mM. This increase in $[K^+]_o$ is similar to the increase that occurs in the subretinal space of the intact vertebrate eye during a transition from light to dark (Steinberg et al., 1985). The $[K^+]_o$-induced changes in RPE cell volume are similar in magnitude and time course to the light-induced changes in subretinal space volume recently reported by Huang and Karwoski (1989). RPE cell volume regulation could therefore play an important role in controlling the chemical composition of the subretinal space and might also provide a mechanism for maintaining the normal adhesivity between RPE and retina. Some of this work has been presented previously in abstract form (Adorante and Miller, 1989).

METHODS

Bullfrogs (*Rana catesbeiana*) were obtained from Western Scientific (Sacramento, CA), kept in running tap water at room temperature for 1 wk or more before use, and fed live crickets daily. The composition of the standard Ringer bathing solution was (in mM): 82.5 NaCl, 27.5 $NaHCO_3$, 2 KCl, 1 $MgCl_2$, 1.8 $CaCl_2$, and 10 glucose. Tetramethylammonium (TMA) chloride loading solution (TMACl) was made by equimolar replacement of 50 mM Na with TMA. Zero Na solutions were made by isosmotic replacement of Na with *N*-methyl-D-glucamine salts of Cl and HCO_3. Na cyclamate was used in place of NaCl when $[Cl]_o$ was reduced in the bathing medium. All HCO_3-containing media were saturated with a 95% O_2–5% CO_2 gas mixture (pH = 7.4). The composition of the nominally HCO_3-free Ringer (HEPES buffer) was (in mM): 82.5 NaCl, 4.2 NaHEPES, 5.9 HEPES, 17.5 Na cyclamate, 2.0 KCl, 1.0 $MgCl_2$, 1.8 $CaCl_2$, and 10 glucose (pH = 7.4). Bumetanide was a gift from Hoffman–La Roche (Rahway, NJ).

The osmolality of all solutions was measured using a freezing point depression osmometer (Advanced Wide-Range Osmometer 3W2; Advanced Instruments, Inc., Needham Heights, MA). Control Ringer osmolality was 230 ± 3 mosmol/kg. Hyperosmotic solutions of 255 ± 3 and 280 ± 3 mosmol/kg were made by the addition of mannitol to control Ringers.

Electrophysiology

The RPE-choroid was isolated as described previously and mounted in an Ussing-type chamber that allowed the two sides of the tissue to be perfused independently (Miller and Steinberg, 1977*a*). Solutions were delivered to the chamber by CO_2-impermeable Saran tubing (Clarkson Equipment and Control, Detroit, MI). The solution reservoirs and the chamber were separated by an open manifold (250 μl) that served to maintain a constant

hydrostatic head during solution changes (Joseph and Miller, 1990). Because the solution changes were made at the manifold, there was a 20–45-s delay before the dead space cleared and the new solution reached the tissue. The rate of fluid exchange in the chambers was 10–30 vol/min, depending on the flow rate. In all figures, the horizontal bar indicates when solution changes were made at the manifold.

The recording circuitry has been described previously (Hughes et al., 1988). Ringer agar bridges in the apical and basal baths made electrical contact with nearby calomel electrodes and the transepithelial potential (TEP), referenced to the basal bath, was recorded differentially between the calomel electrodes. Apical and basolateral membrane potentials, V_a and V_b, respectively, were recorded using the conventional barrel of the double-barreled microelectrode referenced to the calomel electrodes. The output signal from the double-barreled microelectrode ($V_1 - V_a$) was obtained from the difference in the voltage outputs of the resin containing barrel (V_1) and the conventional barrel (V_a), both referenced to the apical bath. All voltage signals were digitized and stored on a microcomputer for later analysis.

Double-barreled K^+-selective Microelectrodes

The fabrication and calibration of double-barreled K^+-selective microelectrodes was previously described in some detail (Hughes et al., 1988). Very similar procedures were used in the present experiments to make the intracellular TMA^+ concentration measurements.

In brief, we used thick septum theta glass from WPI (New Haven, CT) and the active barrel was silanized using a modification of the technique of Coles and Tsacopoulos (1977). The micropipettes were dried in a small oven at 250°C for ~1.25 h and ~100 μl of trimethyldimethylsilamine (TMSDMA) was then added for 40–45 min. The oven was vented and the electrodes were baked for an additional 1.25 h at 250°C. After the microelectrodes cooled, the silanized barrel was filled using a K ion-exchange resin (477317; Corning Glass Works, Corning, NY) and backfilled with 150 mM KCl. The reference barrel was filled with 150 mM Li acetate plus 1 mM KCl. The resistance of the ion-specific barrel was 10–30 GΩ. The reference barrel varied from 125 to 175 MΩ.

Double-barreled K^+-resin microelectrodes were calibrated before and after an experiment using a series of TMA-containing solutions ranging from 1 to 20 mM in a background of 120 mM KCl. The voltage response was a linear function of the log $[TMA^+]$ concentration between 1.0 and 20 mM TMACl. The electrode slope was determined by linear regression analysis. It was 56.8 ± 0.4 mV (mean ± SEM, $n = 57$). The TMA^+ to K^+ selectivity was ~750:1.

The acceptance criterion for the reference barrel was that the tip potential between control Ringer and the 120 mM KCl solution be <5 mV. The electrodes were recalibrated after each experiment, and if the slopes were not within 5 mV of the initial calibration the data were discarded.

Measurement of Cell Volume Changes Using TMA-loaded Cells

As shown by Reuss (1985), changes in the volume of *Necturus* gallbladder epithelial cells can be measured electrophysiologically by first loading the cells with a probe, TMA^+. Pretreatment of the apical membrane with nystatin was required to load these cells with TMA^+. After the subsequent withdrawal of nystatin the apical membrane permeability and voltage returned to normal and the TMA^+ was trapped within the cells (Cotton et al., 1989).

A K^+-specific microelectrode based on the liquid resin exchanger potassium tetrakis (*p*-chlorophenylborate) was then used to measure changes in $[TMA^+]_i$. This measurement is possible, despite high levels of $[K^+]_i$, because the resin is approximately three orders of magnitude more sensitive to TMA^+ than K^+ (Neher and Lux, 1973). Thus, small amounts of

$[TMA^+]_i$ provide an impermeant intracellular volume marker and the changes in $[TMA^+]_i$ signal can be used to monitor changes in cell water.

In the present experiments a slightly different procedure was used because we found that nystatin was not needed to permeabilize the RPE apical membrane. Fig. 1 *A* shows that isosmotic addition of 50 mM TMA^+ (Na replacement) to the apical bath increase $V_I - V_a$ by ~134 mV, from 62 to 196 mV. This increase occurred over 12 min and corresponded to a cell TMA concentration of ~20 mM. In 39 cells (39 tissues) the steady level of $\Delta(V_I - V_a)$ was 128.4 ± 2.1 mV (mean ± SEM), which corresponds to a $[TMA^+]_i$ concentration of 17.9 ± 2.9 mM.

In a series of preliminary experiments (not shown) we observed that removal of TMA^+ from the extracellular bath resulted in a slow (~60 min) dissipation of the $[TMA^+]_i$ signal, which was prevented by having 2 mM TMA^+ present in the apical bath after the loading phase. After a brief equilibration period (30 min, Fig. 1 *A*) the TMA^+ signal remained elevated and constant for hours over many cell impalements. Consequently, all control and experimental media after the TMA^+-loading phase contained 2 mM TMA^+.

The choice of 2 mM extracellular TMA^+ was somewhat arbitrary. For example, after TMA^+ loading and equilibration subsequent changes in extracellular TMA^+, between 2 and 1 mM, had practically no effect on the $[TMA^+]_i$ signal ($n = 2$, not shown). However, lowering apical $[TMA^+]_o$ by a factor of 10, from 1 to 0.1 mM, caused the $V_I - V_a$ signal to decrease by ~3 mV in 7 min. The return to 2 mM $[TMA^+]_o$ completely reversed this decrease and provided a constant intracellular signal. These results demonstrate that a small amount (1–2 mM) of extracellular TMA^+ is sufficient to maintain an intracellular concentration of 15–20 mM.

In comparison to the apical changes, isosmolar addition of 50 mM TMA^+ to the basal bath had practically no effect on the cellular accumulation of TMA, 100–200 μM in 30 min. In some experiments it was technically convenient to have 2 mM TMA^+ present in both apical and basal perfusates after the TMA^+ loading phase. No differences were noted when compared with identical experiments in which 2 mM TMA^+ was present in the apical bath only.

The lower panel of Fig. 1 *A* shows that TMA^+ addition to the apical bath is associated with a small (2–3 mV) depolarization of the apical (V_a) and basolateral (V_b) membrane potentials. The increase in TEP shows that the depolarization was somewhat larger at the basolateral membrane. These voltage changes could have been produced in several ways. For example, the reduction of apical [Na] causes a liquid junction potential at the agar-filled voltage reference bridge in the apical bath. This is observed as an apparent depolarization of the apical membrane. In addition, previous experiments indicated that $[Na]_o$ reduction produced a paracellular diffusion potential that hyperpolarized V_a and depolarized V_b. In those experiments it was also shown that the apical membrane contains an electrogenic $NaHCO_3$ cotransporter that depolarizes in response to a change in its equilibrium potential after apical [Na] reduction (Hughes et al., 1989). Finally, a TMA^+ diffusion potential could have contributed to the depolarization of V_a. The small secondary change in V_b (TEP increase) suggests that the change in TEP after TMA^+ addition to the apical bath is not solely due to a paracellular diffusion potential.

Stability and Magnitude of the $[TMA]_i$ Signal

In these experiments there was no appreciable electrode drift, or leakage of TMA^+ from the cells, during the time required for volume regulation (≤10 min). This is illustrated in Fig. 1 *B*, which compares the stability of the $[TMA^+]_i$ signal from an impaled cell (lower trace) with the signal from the same electrode, located in the extracellular bath that contained 2 mM TMA (upper trace). In the extracellular bath the drift of the electrode was <0.5 mV/h. The drift of the same electrode, in the cell, was <0.25 mV/h (lower trace). In some instances there was

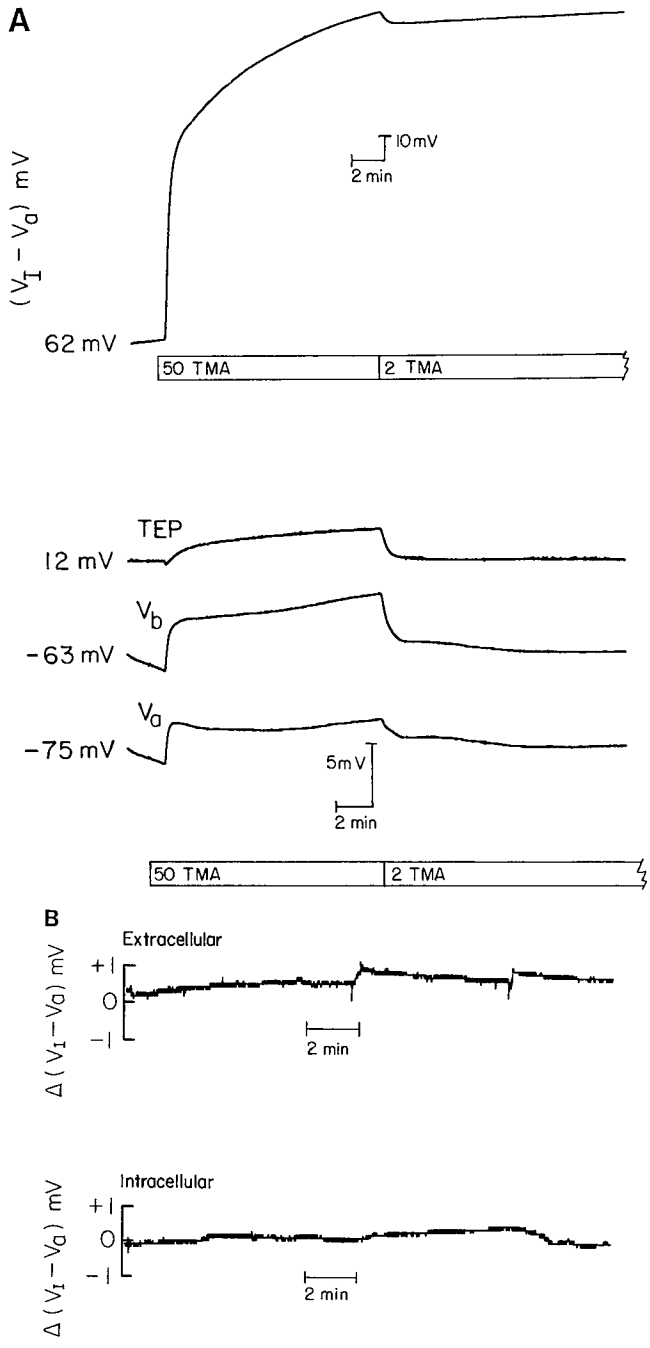

FIGURE 1. Loading bullfrog RPE cells with TMA^+. Values to the left of each trace denote voltages at the start of a record. The signal detected by the ion-specific barrel ($V_I - V_a$) is the difference in the voltage outputs of the ion-specific barrel (V_I) and conventional (V_a) microelectrodes, each referenced to the apical bath. TEP, V_a, and V_b indicate transepithelial, apical, and basal membrane potentials, respectively. (*A*) At the left-most end of the horizontal bar the control Ringer in the apical bath was replaced at the manifold (see Methods) by one containing 50 mM TMA^+ (TMA^+ replaced Na on an equimolar basis). At the second bar the Ringer was replaced by one containing 2 mM TMA^+. Perfusion with 50 mM TMA caused a rapid increase in $V_I - V_a$ equivalent to a cellular TMA^+ ($[TMA^+]_i$) concentration of ~20 mM. This level is maintained by 2 mM TMA^+ in the apical bath after TMA^+ loading. The intracellular signal ($V_I - V_a$) before TMA^+ loading is due to the presence of cell K^+, which the ion-specific barrel senses in the absence of $[TMA^+]_o$. The bottom panel shows the changes in TEP, V_a, and V_b that accompany the above solution changes. (*B*) The stability of the TMA^+ signal compares favorably with the electrode signal drift. The upper trace shows the TMA^+ signal when the electrode is immersed in the extracellular bath that contains 2 mM TMA^+. The lower trace shows the TMA^+ signal after cell impalement using the same electrode. It shows that TMA^+ leakage from the TMA^+-loaded cells is negligible under control conditions.

virtually no drift in the TMA^+ signal of an impaled cell for >30 min. In contrast, the changes in the TMA signal that occurred as a result of the imposed changes in cell volume were 2–5 mV in magnitude (see Figs. 4 *A* and 5). Additionally, the TMA^+ signal from osmotically shrunken cells in the presence of 2 mM K^+ in the apical bath remained elevated and did not decrease for as long as an impalement could be maintained (>30 min; Fig. 3 *A*). Therefore, electrode drift or leakage of TMA^+ out of the cells are not significant factors in these experiments.

In Figs. 3–8 the changes in cell volume are plotted as a function of time relative to the isosmotic control volume, denoted as 1.00 on the ordinate. The cell volume ratio or relative cell volume (V_t/V_o) is given by the following relationship:

$$V_t/V_o = 10^{(E_o - E_t)/S}, \quad (1)$$

where S is the slope of the electrode, E_o is the electrode signal under control conditions ($= V_I - V_a$) in millivolts, E_t is the signal at any time (t) after a change in solution osmolality, V_o is the control volume, and V_t is the cell volume at any time (t). A 1-mV change in ($V_I - V_a$) corresponds to a ~4% change in cell water volume (see below).

Cell volume is determined by the amount of cell water (variable) and cell solids (constant). Changes in $[TMA^+]_i$ reflect changes in cell water content (V_w), the osmotic component of cell volume. It follows that this method measures changes in cell water volume.

In most cases the regulatory volume increase after osmotic cell shrinkage was a linear function of time (see Figs. 4 and 5). The rate of cell volume increase (recovery) was obtained by measuring the slope of the best-fitting straight line drawn through the initial portion (first 30–60 s) of the reswelling curve.

Validity of Measurements of RPE Cell Volume Changes: Initial and Secondary

If we assume that the RPE cell membranes have a very large water permeability as demonstrated in a number of epithelia (Larson and Spring, 1987), then the cell osmolality will always be equal to that of the medium. If cell solute remains constant after an osmotically induced change in cell volume, then according to the Boyle–van't Hoff relationship $\pi_2/\pi_1 = V_1/V_2$, where the cell water volumes, V_1 and V_2, correspond to a medium osmolality of π_1 and π_2, respectively (House, 1976). Cell volume changes that follow the Boyle–van't Hoff relationship are said to be osmometric.

The rapid increase in the TMA^+ signal (<60 s) after an increase in apical bath osmolality is consistent with the assumption that the apical membrane water permeability is high (see Fig. 3). The calculated osmometric decrease in cell volume during the rapid shrinkage phase suggests that cell solute remained constant. From these observations it follows that the change in the TMA^+ signal accurately reflects initial rapid changes in cell volume.

Accurate determination of secondary changes in cell volume (i.e., cell volume regulation) depends on whether the cell content of TMA^+ remains constant relative to the time it takes for the cells to regulate their volume. Fig. 3 shows that an increase in apical bath osmolality causes the TMA^+ signal to increase (cell volume decrease) and remain elevated until the osmotic pulse is removed. Under these conditions the TMA^+ signal remains elevated and constant for as long as the impalement can be maintained (>30 min). This is well beyond the time required for the RPE cells to regulate their cell volume back to control level (3–10 min in most cases). These results also indicate that TMA^+ does not leak out of the cells after osmotic shrinkage.

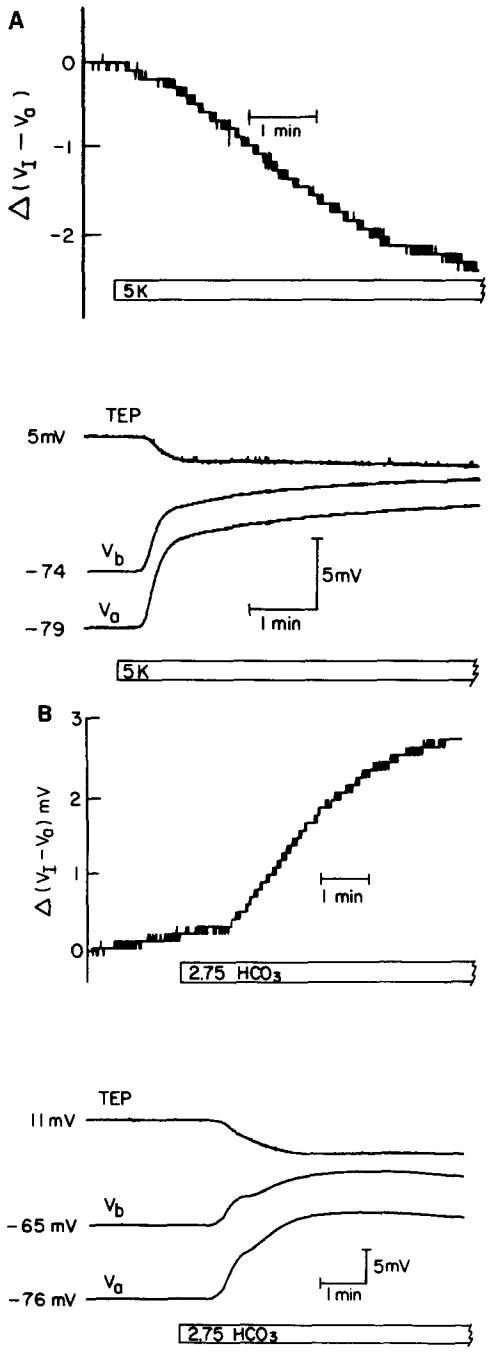

FIGURE 2. Changes in $[TMA]_i$ and V_a after an increase in apical $[K^+]$ (*A*) or a decrease in $[HCO_3]$ (*B*). (*A*) At the horizontal bar the control Ringer at the apical bath was switched to one containing 5 mM $[K^+]_o$. Elevation of apical $[K^+]$ depolarized V_a by ~7 mV and V_b by ~5 mV and decreased TEP (*bottom*). Concomitant with these voltage changes $V_I - V_a$ decreased by ~2.0 mV. Bottom panel shows the changes in TEP, V_a, and V_b resulting from the solution changes. Ordinate of upper panel shows relative change in TMA^+ signal Δ $(V_I - V_a)$ after apical $[K^+]$ addition or $[HCO_3]$ reduction. (*B*) At the horizontal bar the control Ringer at the apical bath was switched to a solution containing 2.75 mM HCO_3. After HCO_3 reduction V_a and V_b initially depolarized by ~13 and 8 mV, respectively (*bottom*). In this case $V_I - V_a$ increased by ~2.4 mV (*top*).

Possible Mechanisms of TMA^+ Uptake

The mechanism(s) for TMA^+ uptake at the apical membrane is unknown. A variety of cation transport mechanisms, located at the RPE apical membrane, were examined for their possible involvement in TMA^+ uptake. They include an electrogenic Na/K pump, a large Ba^{2+}-inhibitable K^+ conductance, an electrogenic DIDS-inhibitable $NaHCO_3$ cotransporter, and a bumetanide-sensitive Na,K,Cl cotransporter (Miller and Steinberg, 1977*a*; Miller et al., 1978; Hughes et al., 1988, 1989; Joseph and Miller, 1990; Miller and Edelman, 1990).

We tested a number of inhibitors that block these transport mechanisms to see if they could block the uptake of TMA^+ during the loading phase. Neither Ba^{2+}, DIDS, nor bumetanide had any effect on TMA^+ loading of the RPE cells. The same steady-state cell $[TMA^+]_i$ level was achieved in all cases. This eliminates K^+ channels, the $NaHCO_3$ cotransporter, and, most importantly, the bumetanide-sensitive Na,K,Cl cotransporter as the source of TMA^+ entry. Inhibition of the Na/K pump by removal of apical $[K^+]$ and inhibition of the $NaHCO_3$ cotransporter by $[HCO_3]_o$ removal were equally ineffective. 1 mM amiloride also failed to inhibit TMA^+ uptake, indicating that TMA^+ is not likely to be mediated by a TMA^+/H^+ exchange or an amiloride-inhibitable Na channel. The absence of a change in cell pH after the addition of TMA^+ to the apical bath also indicates the absence of an apical TMA^+/H^+ exchange mechanism (Lin, H., and S. S. Miller, unpublished observations). It is therefore unlikely that any of these transporters are responsible for net TMA^+ uptake. It is possible that the net TMA^+ uptake is through a yet unspecified organic cation pathway.

Since many of our experimental manipulations result in the alteration of apical and basolateral membrane potentials, we examined the possibility that in addition to changes in cell volume, membrane potential changes by themselves could alter intracellular TMA^+ activity. In Fig. 2 *A* the cells were first loaded with TMA^+ and then apical $[K^+]$ was elevated from 2 to 5 mM by the replacement of Na by K (open bar, upper and lower panels). Because the apical membrane of the frog RPE has a large K^+ conductance, elevation of apical $[K^+]$ causes the apical membrane to depolarize (Miller and Steinberg, 1977*a*). Electrical coupling through a paracellular pathway also causes V_b to depolarize to a lesser extent. After the depolarization of V_a and V_b the TMA^+ signal decreased by ~2.4 mV in ~3 min (-1.9 ± 0.2 mV; mean ± SEM; $n = 7$ cells and 7 tissues). This decrease in $V_I - V_a$ is equivalent to an ~10% increase in cell volume resulting from the stimulation of net solute uptake at the apical membrane (see Results).

In contrast, when the apical and basal membranes were depolarized, by reducing apical HCO_3 (at constant P_{CO_2}; Fig. 2 *B*), $V_I - V_a$ increased by ~2.5 mV (2.1 ± 0.1 mV; $n = 4$ cells and 3 tissues). Reducing apical HCO_3 decreases the driving force on the apical membrane electrogenic $NaHCO_3$ cotransporter and therefore reduces net solute uptake (Hughes et al., 1989). Reduction of net solute uptake will tend to decrease cell volume and therefore increase $V_I - V_a$. Taken together these observations strongly suggest that changes in membrane voltage per se do not alter $[TMA]_i$.

RESULTS

Hyperosmotic Cell Shrinkage

To determine whether the bullfrog RPE could regulate its cell volume after osmotic shrinkage, the apical bath osmolality was increased by adding mannitol to control Ringers. Fig. 3 *A* shows that the addition of 25 mM mannitol to the control 2 mM $[K^+]_o$ Ringer in the apical bath caused a rapid increase in the TMA^+ signal of ~2.8 mV (left ordinate), which is equivalent to a decrease in cell volume of ~10% (right ordinate). In 10 cells from 10 tissues the decrease in cell volume was $-11.0 \pm 0.6\%$

(mean ± SEM). The initial rapid rise in the TMA^+ signal in Fig. 3 *A* (~30 s) is followed over the next 8 min by a much slower secondary increase in the TMA^+ signal (cell shrinkage). In 10 cells from 10 tissues this secondary shrinkage accounted for an additional 4.3 ± 0.8% cell volume decrease (mean ± SEM). This secondary phase suggests that the cells lost solute during this period.

The decrease in relative cell volume or cell volume ratio (V_t/V_o; see Methods) that occurred during the rapid initial shrinking phase is equal to the ratio π_1/π_2, where π_1 and π_2 are the apical bath osmolalities before and after the addition of mannitol. Thus the cell initially shrinks as a perfect osmometer.[1] Removal of the osmotic pulse (at $t = 9$ min) caused the cell TMA^+ signal to rapidly decrease (cell volume increased) to a value that is above control level (left ordinate). The cell did not swell to the same extent as it shrank (cell volume was ~4% below control; right ordinate). This response supports the assumption that the cells lost solute during the secondary increase in the TMA^+ signal (secondary decrease in cell volume; Lohr and Grantham, 1986).

In this class of experiments we could find no evidence for volume regulation after an increase in apical bath osmolality of 25 mosmol using mannitol ($n = 15$ cells and 11 tissues).

The 25-mM osmotic pulse also produced small transient changes in V_a (1 mV or less; $n = 17$ cells and 12 tissues) and even smaller changes in V_b (Fig. 3 *A bottom*) suggesting that these primary effects were at the apical membrane (Miller and Steinberg, 1977*a*). In some instances there was a small (~2 mV) secondary hyperpolarization of V_a and V_b, which appeared to originate at V_a (TEP increased) and followed the time course of secondary cell shrinkage. This secondary hyperpolarization of V_a was more evident using 50 mM mannitol, possibly because of the greater secondary cell shrinkage (Fig. 3 *B*).

Since the rate of cell volume regulation in a number of cell types has been shown to be a monotonic function of the magnitude of cell volume change (Cala, 1986), it is possible that the RPE cells would have performed an RVI had cell volume decreased further.

[1] Because an increase in the osmolality of the apical bath resulted in osmometric cell shrinkage, it is possible that: (*a*) the unstirred layer adjacent to the basal membrane prevents changes in solute/solvent activity from reaching that membrane, and/or (*b*) the apparent permeability of the basolateral membrane is low relative to the apical membrane. This may be the result of a difference in hydraulic water conductivities (L_p's) or a difference in membrane surface areas (Larson and Spring, 1987). Although the unstirred layer adjacent to the basolateral membrane is a barrier, the basolateral membrane potential can still respond to changes in the ionic composition of the bath (Miller and Steinberg, 1977*a*). For example, when $[K^+]$ is elevated in the basal bath from 2 to 12 mM, V_b depolarizes by 15–20 mV within 2–3 min of the solution composition change (unpublished observations). Therefore, although the unstirred layer impedes solute movement, it does not prevent a solution composition change from reaching the basolateral membrane. On the other hand, changing the osmolality of the basal bath by ±50 mosmol/kg (not shown) failed to produce any significant change in cell volume. Therefore, unstirred layer effects cannot account for osmometric cell shrinkage after an increase in apical bath osmolality or the absence of cell volume changes after changes in basal bath osmolalities. In the bullfrog RPE the area of the apical membrane is at least 10 times its basal surface area (Miller and Steinberg, 1977*a*). Assuming equal L_p's for apical and basal membranes, the osmolality of the bath facing the membrane with the greater surface area will tend to determine cell volume.

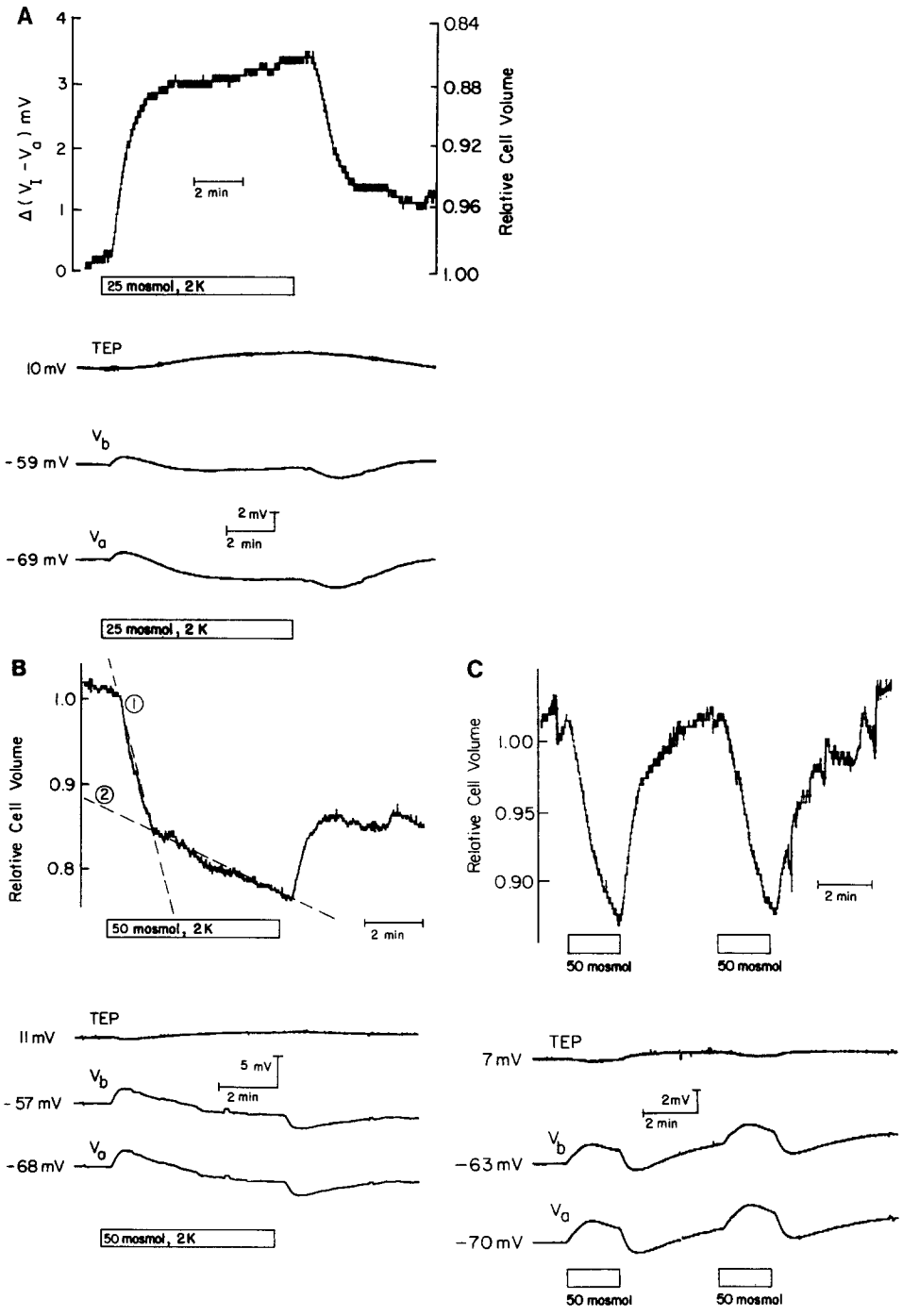
A
Δ(V_I - V_a) mV
Relative Cell Volume
2 min
25 mosmol, 2K
TEP
10 mV
V_b
-59 mV
2 mV
2 min
V_a
-69 mV
25 mosmol, 2 K
B
Relative Cell Volume
50 mosmol, 2K
2 min
TEP
11 mV
5 mV
2 min
V_b
-57 mV
V_a
-68 mV
50 mosmol, 2K
C
Relative Cell Volume
2 min
50 mosmol
50 mosmol
TEP
7 mV
2mV
2 min
V_b
-63 mV
V_a
-70 mV
50 mosmol
50 mosmol

FIGURE 3.

In another tissue (Fig. 3 *B*) the RPE cells were shrunken to a greater extent by the addition of 50 mM mannitol to the apical bath. These experiments also showed two distinct phases of cell shrinkage after an increase in apical bath osmolality with mannitol. A rapid osmometric cell shrinkage (first phase) of ~18% (−16.6 ± 0.7%; mean ± SEM $n = 10$ cells and 7 tissues), was followed by a much slower secondary shrinkage of ~12% (−10 ± 2.6%; $n = 7$ cells and 7 tissues). The cell did not reswell until control Ringer was returned to the apical bath. This caused a rapid cell swelling, but to a level below control, consistent with cell solute loss during the secondary cell shrinkage phase. Thus, despite the larger osmotic stimulus when compared with Fig. 3 *A*, the cells still failed to regulate their volume after hyperosmotic mannitol addition.

In Fig. 3 *C* we examined the initial osmotic phase of cell shrinkage by limiting the exposure time to the hyperosmotic pulse. In this case the osmotic pulse (50 mM) was on for only 2 min. Osmometric changes in cell volume were seen for both cell shrinkage after the osmotic pulse and cell swelling following its removal ($n = 3$ cells and 3 tissues). An identical response could be reproduced minutes later. In this class of experiments the secondary shrinkage phase seen in Fig. 3, *A* and *B* was absent, presumably because the cells had not lost solute in this short period of exposure.

Apical [K]-induced Volume Regulation

In some cell types, cell reswelling (regulatory volume increase) does not follow hyperosmotic shrinkage unless extracellular [K^+] is elevated to 10–15 mM (Kregenow, 1971; Hoffman and Simonsen, 1989). In contrast to the experiments of Fig. 3, *A* and *B*, Fig. 4 shows that these cells can reswell after osmotic shrinkage if apical [K^+] is elevated concomitant with the osmotic pulse.

In the experiments of Fig. 4 the apical bath osmolality was increased 50 mosmol/kg by the addition of 36 mM mannitol and 8 mM KCl ($[K^+]_o = 10$ mM). This maneuver resulted in a rapid cell shrinkage of ~14% (−13 ± 2%; mean ± SEM; $n = 5$ cells and 5 tissues). Rapid cell shrinkage was followed by a slower reswelling back to control value (~5 min; rate of volume recovery = 3.4 ± 0.4%/min; mean ± SEM; $n = 5$ cells and 5 tissues). The initial rapid cell shrinkage was slightly

FIGURE 3. (*opposite*) Changes in RPE cell volume after hyperosmotic addition of mannitol to the apical bath. (*A*) *Top*, Left ordinate shows the change in cell TMA^+ signal $\Delta(V_1 - V_a)$ mV after 25 mM mannitol addition and removal from the apical bath; right ordinate is the calculated change in cell volume (1 mV change in $V_1 - V_a$ ~4% change in cell volume; see Methods). Note the reciprocal relationship of $\Delta (V_1 - V_a)$ and cell volume. *Bottom*, Changes in V_a, V_b, and TEP associated with hyperosmotic mannitol addition and removal. The beginning and end of the horizontal bar indicate the onset and removal of 25 mM hyperosmotic pulse. (*B*) Changes in cell volume after a 50 mosmol/kg increase in apical bath osmolality. *Top*, Ordinate depicts the calculated relative change in cell volume (see Methods). At $t = 0$ the relative cell volume is designated as 1.00 unless otherwise specified. *Bottom*, Changes in TEP, V_a, and V_b. Increasing apical bath osmolality by 50 mosmol/kg using mannitol resulted in two phases of cell shrinkage. The osmometric phase is denoted by 1 and the secondary cell shrinkage phase is denoted by 2. (*C*) Brief (2 min) hyperosmotic pulses (*open bar*) yielded reproducible osmometric decreases in cell volume with no secondary cell shrinkage.

less than osmometric. Perfect osmotic shrinkage would result in a ~16–20% cell volume decrease. This range reflects the precision of the osmotic measurements (see Methods).

The initial rapid depolarizations of V_a and V_b that accompany cell shrinkage are the result of an increase in $[K^+]_o$, which changes E_K at the apical membrane. Electrical coupling through the paracellular shunt caused the smaller depolarization of V_b (Miller and Steinberg, 1977*a*).

The experiments of Fig. 4 suggest that the bullfrog RPE cells regulate their volume after osmotic shrinkage by a K^+-dependent transport mechanism. However, when apical $[K^+]$ was isosmotically increased from 2 to 5 mM the cells swelled, within 10–30 min, to a new steady-state volume that was 7.1 ± 1.9% (mean ± SEM; 12 cells

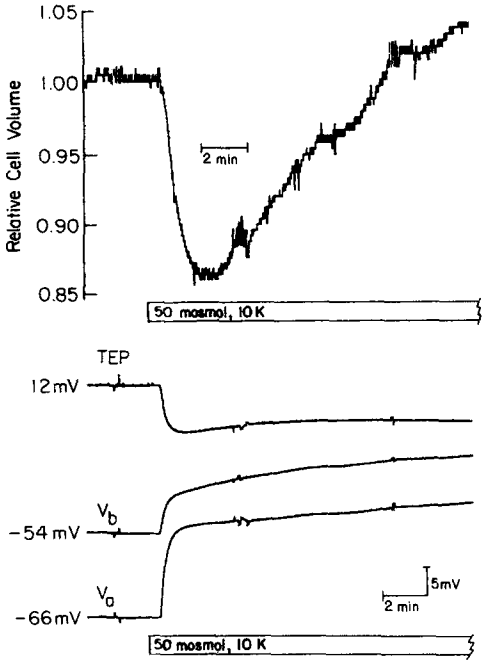

FIGURE 4. Osmotic shrinkage is followed by cell reswelling in the presence of elevated apical $[K^+]$. At the horizontal bar the control Ringer was replaced with one made hyperosmotic by the addition of mannitol and KCl. (KCl was increased by 8 mM and 34 mM mannitol was added to raise the osmolality by 50 mosmol/kg.) The depolarization of V_a and V_b (*bottom*) is the result of a change in E_K at the apical membrane after the increase in $[K^+]_o$.

and 10 tissues) above control (not shown). Thus it is possible that the cell reswelling seen in Fig. 4 was the result of a change in the force (thermodynamic effect) driving some steady-state transport mechanism obligatorically coupled to K^+ (or one that responds to $[K^+]_o$-induced membrane potential changes) as opposed to volume-dependent activation of a volume regulatory transport mechanism (a kinetic effect).

To distinguish between a volume-activated solute uptake mechanism and one that responds solely to a change in its driving force, $[K^+]_o$ was raised *before* the hyperosmotic pulse.

In the experiment shown in Fig. 5, apical $[K^+]$ was elevated 15 min before hyperosmotic addition of 25 mM mannitol. During this period the cell swelled to a new steady-state volume that was ~5% above control. A switch to hyperosmotic

Ringer was followed by a rapid cell shrinkage (<1 min) and a slower cell reswelling to control volume in ~8 min. These results, summarized in Table I, are consistent with volume-dependent activation of a volume regulatory process that is dependent on apical $[K^+]$.

Fig. 5, *bottom* shows the voltage changes associated with the changes in cell volume. The changes that occur in both V_a and V_b (1 mV or less) are small and transient. In some cases there is a slow secondary depolarization of V_b (1–2 mV) during the regulatory phase (see Discussion).

Table I shows that osmotic shrinkage of bullfrog RPE cells in HCO_3-free Ringer with 5 mM apical $[K^+]$ was similar to that in HCO_3-containing media. These observations eliminate the apical $NaHCO_3$ cotransporter as a major contributor to

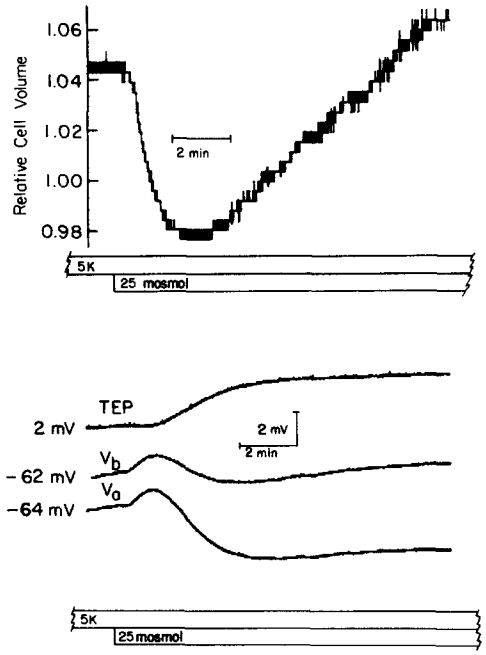

FIGURE 5. The effect of elevating apical $[K^+]$ from 2 to 5 mM before an increase in apical bath osmolality (25 mM mannitol). Approximately 15 min before mannitol addition (upper horizontal bar), apical $[K^+]$ was isosmotically raised to 5 mM. At the start of the lower horizontal bar the apical bath osmolality was increased 25 mosmol/kg using mannitol. Despite the continued extracellular hyperosmolality the cell reswelled to control level. *Top*, Relative cell volume. Note the higher starting cell volume ($t = 0$), indicating that cell swelling occurred during isosmotic elevation of apical $[K^+]$ (see Results). *Bottom*, Changes in TEP, V_a, and V_b induced by cell shrinkage and reswelling.

RVI since this mechanism has a K_m for HCO_3 in the millimolar range (Hughes et al., 1989).

Ionic Dependence of RVI

It has been shown that the RPE apical membrane contains a bumetanide-sensitive Na,K,Cl cotransporter that is responsible for net K and Cl transport across the epithelium (Miller and Edelman, 1990; Edelman et al., 1988; Joseph and Miller, 1990). Because of the $[K^+]_o$ requirement for RVI it was important to test whether this mechanism could also regulate cell volume.

TABLE I

Rate of Cell Swelling (RVI) after Addition of 25 mM Mannitol to the Apical Bath

Treatment	Rate of volume recovery	Cells (tissues)
	%/min	
Control	3.0 ± 0.2	16 (12)
0 mM Na	0.1 ± 0.1	3 (3)
2 mM Cl	0.5 ± 0.3	4 (3)
Bumetanide	0.2 ± 0.2	4 (3)
HEPES	3.4 ± 0.4	7 (6)

Effect of Na removal, Cl reduction, and bumetanide on RVI. The table summarizes the experiments of Figs. 5–8. Rate of recovery is expressed as mean percent volume increase per minute ± SEM.

If the Na,K,Cl cotransporter contributes to cell volume regulation, then RVI should be inhibited or its rate reduced when either Na or Cl in the apical bath is reduced, since they contribute to the driving force for this mechanism. Further, bumetanide, a known inhibitor of Na,K,Cl transport in epithelia, should also inhibit RVI (O'Grady et al., 1987). The experiments presented below (Figs. 6–8) test the hypothesis that Na,K,Cl cotransport mediates RVI in the bullfrog RPE.

Fig. 6 shows the effect of Na removal from the apical bath on RVI. Na was removed and $[K^+]_o$ was isosmotically raised to 5 mM before the osmotic challenge. After Na removal from the apical bath, the cell volume was reduced ~12–15% below control levels (n = 7 cells and 7 tissues). This shrinkage may be attributed to the

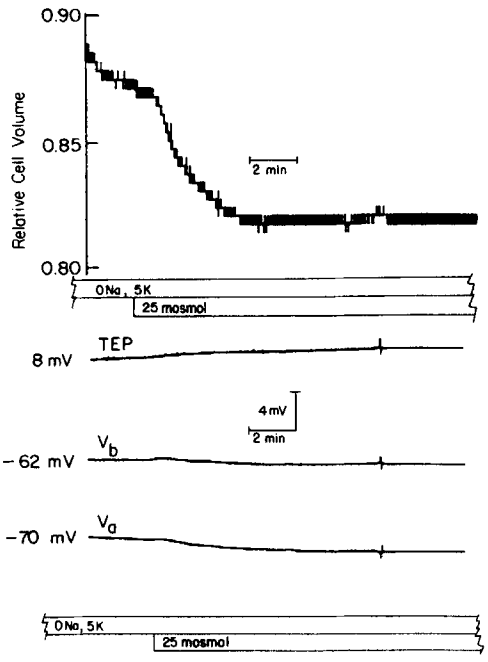

FIGURE 6. Apical Na removal inhibits RVI. The upper bar denotes the removal of apical Na (NMDG substitution) and the elevation of $[K^+]_o$ to 5 mM 15 min before mannitol addition (lower bar). At t = 0 cell volume was reduced by ~13%, presumably due to prior Na removal (see Results). The lower panel shows that hyperosmotic changes in voltage were blunted by Na removal from the apical bath.

reversal or inhibition of two apical membrane solute uptake mechanisms (see Discussion). At the time indicated (lower bar) the apical bath was made hyperosmotic by addition of 25 mM mannitol. Under these conditions the cells shrank and remained shrunken (Table I). Thus RVI requires apical Na.

The voltage changes associated with hyperosmotic exposure were virtually abolished in the absence of Na in the apical bath (see Discussion).

The Cl dependence of the RVI was examined in the experiment summarized in Fig. 7. In this experiment $[K^+]_o$ was increased to 5 mM, and Cl was isosmotically reduced in the apical bath from 90 to 2 mM 15 min *before* osmotic shrinkage. Although a small increase in cell volume (<2% in this experiment) followed cell

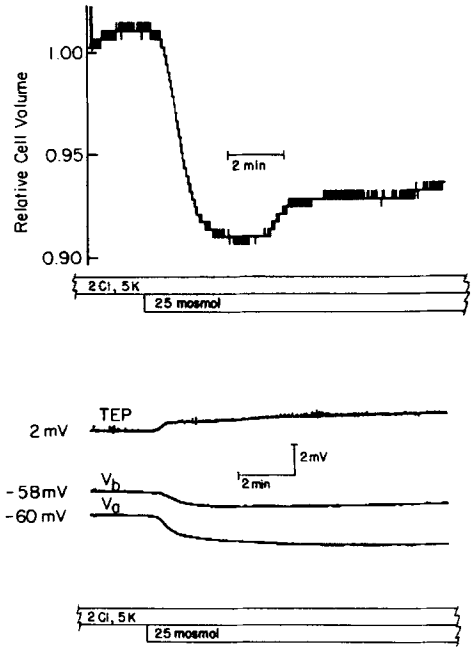

FIGURE 7. Apical Cl reduction inhibits RVI. $[K^+]_o$ was elevated to 5 mM and [Cl] was reduced from 90 to 2 mM (broken horizontal bar) 15 min before the addition of 25 mM mannitol to the apical bath. At the lower horizontal bar the apical bath was made hyperosmotic by addition of mannitol. The hyperosmolality-induced changes in membrane voltage are shown below.

shrinkage, this did not always occur and is not significant (Table I). RVI therefore also requires the presence of apical Cl.

Fig. 7, *bottom* shows the voltage changes after the hyperosmotic pulse in the low Cl medium. Small hyperpolarizations of V_a and V_b occurred (<2 mV). The voltage response probably originated at the apical membrane as suggested by the increase in TEP that occurred during the hyperpolarization of V_a and V_b (Miller and Steinberg, 1977*a*). These voltage responses were variable, and in some cases small, transient depolarizations were seen.

The bumetanide sensitivity was tested in the experiments of Fig. 8, where $[K^+]_o$ was increased isosmotically to 5 mM and 0.1 mM bumetanide was added to the apical

bath ~15 min before increasing the bath osmolality by 25 mosmol/kg.[2] Fig. 8 shows that RVI was greatly inhibited despite the presence of elevated $[K^+]_o$. The rate of cell volume recovery in the presence of bumetanide was only ~6% of control (Table I). When the apical bath was subsequently perfused with control Ringer the cells rapidly returned to control volume.

The electrical responses of V_a and V_b after an osmotic pulse were small (<2 mV; Fig. 8, *bottom*) and variable in the presence of elevated $[K^+]_o$ and bumetanide. The reduced TEP and membrane potentials are the result of increasing $[K^+]_o$ before cell shrinkage. The hyperpolarization of V_a and V_b after the return to control Ringer (2 mM $[K^+]_o$) is the result of a change in E_K at the apical membrane.

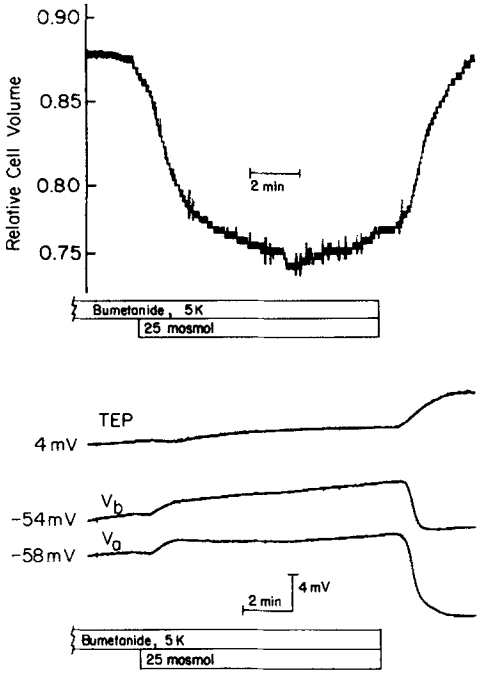

FIGURE 8. Bumetanide inhibits RVI. 0.1 mM bumetanide was added and $[K^+]_o$ was increased in the apical bath to 5 mM (upper broken horizontal bar) 10 min before hyperosmotic mannitol addition (lower horizontal bar). *Top*, Relative cell volume. The lower starting cell volume ($t = 0$) indicates that cell shrinkage occurred after addition of bumetanide to the apical bath. The lower panel shows the changes in TEP, V_a, and V_b resulting from mannitol addition in the presence of apical bumetanide.

Thermodynamic Considerations Favoring 1Na,1K,2Cl Cotransport

The role of $[K^+]_o$ in RVI may be understood on strictly thermodynamic grounds. It has been shown in several systems that the bumetanide-sensitive RVI flux mechanism transports Na, K, and Cl in the ratio of 1:1:2 (O'Grady et al., 1987; Haas, 1989). This is consistent with our observation in the RPE that the bumetanide-sensitive

[2] The presence of bumetanide by itself caused a 10–20% cell shrinkage within 10–15 min ($n = 4$ cells and 3 tissues). In the experiment of Fig. 8, pretreatment with bumetanide caused the cell to shrink by ~10%. The bumetanide-induced cell shrinkage is probably the result of an inhibition of the same net solute uptake mechanism at the apical membrane that mediates RVI (see Discussion).

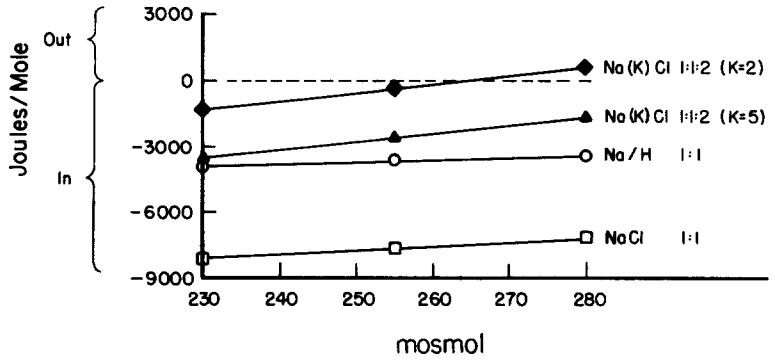

FIGURE 9. Calculated driving forces for Na,K,2Cl ($[K^+]_o$ = 2 mM; 5 mM), Na/H exchange, and NaCl cotransport as a function of medium osmolality. Initial intracellular concentrations of Na, K, and Cl, after hyperosmotic mannitol addition, were calculated by assuming osmometric cell shrinkage. The relative cell volumes at 255 and 280 mosmol/kg are ~0.90 and 0.82, respectively. Multiplication of the measured control intracellular concentrations for Na, K, and Cl by the reciprocal of the relative cell volume yielded the initial cell concentrations at a given osmolality. The intracellular concentrations of $[Na]_i$, $[K]_i$, and $[Cl]_i$ under isosmotic conditions are 14, 110, and 27 mM, respectively (assumed ion activity coefficient, 0.78; Hughes et al., 1987; La Cour, 1989; Fong et al., 1988; our unpublished observations). The value used for intracellular pH was 7.2 (Hughes et al., 1989). In control Ringer the extracellular concentrations of $[Na]_o$, $[K]_o$, and $[Cl]_o$ are 110, 2, and 90 mM, respectively (see Methods). A negative driving force indicates net solute influx, while a positive driving force indicates net solute efflux.

mechanism is electrically silent.[3] The magnitude and direction of the driving force for the above mechanism is (Cala, 1983):

$$\Delta\mu = RT[\mathrm{Ln}(Na_i/Na_o) + \mathrm{Ln}(K_i/K_o) + 2\mathrm{Ln}(Cl_i/Cl_o)], \quad (2)$$

where subscripts i and o signify the intra- and extracellular compartments (see Fig. 9 legend for details).

In the calculations shown in Fig. 9 for Na,K,2Cl cotransport, Na/H exchange, and NaCl cotransport we assumed a linear relationship between flux and driving force. This assumption has been verified for volume and *N*-ethylmaleimide–activated K^+

[3] It has been shown by Haas et al. (1982) in duck red cells that the Na(K)Cl-dependent, bumetanide-sensitive RVI mechanism is electrically silent. This assumption was tested in the RPE by adding 0.1 mM bumetanide to the apical bath. After bumetanide addition there was no immediate change in V_a; instead, there was a slow hyperpolarization of V_b and, due to electrical coupling, a smaller hyperpolarization of V_a. The slow hyperpolarization of V_b after bumetanide addition was due to a reduction in $[Cl]_i$. Since the basolateral membrane possesses Cl channels, the increase in E_{Cl} hyperpolarizes the membrane (Fong et al., 1988). Because of a finite paracellular conductance, current is shunted to the apical membrane, which also hyperpolarizes. Since the hyperpolarization of V_b is greater than V_a (TEP decreases), the response is most likely generated at the basolateral membrane (Miller and Steinberg, 1977*a*). The absence of an immediate change in V_a after apical bumetanide addition indicates that the cotransporter is electroneutral.

flux in Amphiuma red blood cells and Na,K,2Cl cotransport in Erlich cells over a range of driving forces >5,000 J/mol (Geck et al., 1980; Adorante and Cala, 1987). In Fig. 9 the range of driving forces is an order of magnitude smaller (<600 J/mol. Therefore, it seems reasonable to assume that the osmotic perturbations used in the present experiments fall on an approximately linear portion of the flux–driving force curve.

Using the measured ion concentrations for cell and medium Na, K, and Cl (see Fig. 9 legend) we calculate a net inward driving force, favoring net solute uptake, of −1,138 J/mol (1,000 J/mol = 10.4 mV) for Na,K,2Cl transport under isosmotic control conditions (2 mM apical K^+). Increasing the apical bath osmolality with mannitol at constant $[K^+]_o$ (2 mM) initially increases cell ion activities (due to cell shrinkage), leaving bath ion activities unchanged. The driving force for Na,K,2Cl cotransport is near zero (−122 J/mol) and becomes positive (+800 J/mol), favoring net solute efflux, when the osmolality increases to 255 and 280 mosmol/kg, respectively. Under conditions where apical K^+ is 2 mM and bath osmolality is 255 or 280 mosmol/kg, RPE cells do not regulate their volume (Fig. 3, *A* and *B*).

In contrast, in the presence of 5 mM $[K^+]$, a condition that supports RVI (Figs. 4 *A* and 5), the driving force for Na,K,2Cl cotransport is relatively large (>−1,450 J/mol) and inwardly directed at 255 and 280 mosmol/kg (Fig. 9).

The driving forces for two other transport mechanisms that could have mediated RVI, Na/H exchange, and NaCl cotransport are plotted as a function of media osmolality in Fig. 9. Both of these driving forces are large and inwardly directed under control conditions, and are only slightly diminished when apical bath osmolality increases by 50 mosmol/kg. The observation that RVI is absent in a hyperosmotic medium containing 2 mM apical K^+ suggests on thermodynamic grounds that neither Na/H exchange nor NaCl cotransport mediates RVI in the bullfrog RPE.

The above results show that RVI requires apical K, Na, and Cl, and is inhibited by the loop diuretic bumetanide. These observations combined with the thermodynamic calculations strongly suggest that a cotransporter which couples Na, K, and Cl in the ratio of 1:1:2 is the most likely mechanism for RVI in the bullfrog RPE.

DISCUSSION

The present data show that osmotic shrinkage of bullfrog RPE cells is followed by reswelling, provided apical $[K^+]$ is elevated. This increase in apical $[K^+]$ from 2 to 5 mM is in the same range as the increase in subretinal $[K^+]_o$ that occurs during a light to dark transition in the intact vertebrate eye (Steinberg et al., 1985). Cell reswelling after osmotic shrinkage occurred when the apical bath osmolality and $[K^+]_o$ were simultaneously increased or when $[K^+]_o$ was raised before an increase in osmolality (Figs. 4 *A* and 5). In the latter case reswelling cannot be attributed to a change in the driving force of an apical or basolateral membrane transporter functioning in the steady state. Thus bullfrog RPE cells undergo a K-dependent RVI after osmotic shrinkage. Our experiments provide the first demonstration of cell volume regulation in the RPE preparation.

The bumetanide-sensitive mechanism for RVI in the bullfrog RPE is also operative under steady-state conditions (Edelman et al., 1988). Cell shrinkage therefore

stimulates the cotransporter to run faster. In other cell types the transport mechanism(s) mediating RVI are dormant until activated by cell shrinkage (Hoffman and Simonsen, 1989). In this sense the cotransporter regulating cell volume in the RPE is unique.

Evidence for Na(K)Cl Cotransport–mediated RVI

Figs. 5–7 and Table I show that RVI is dependent on apical K, Na, and Cl. It must be mentioned however, that ion requirements for a transport effect do not always prove that the ion in question is a substrate. It is possible that removal of a particular ion changes intracellular pH, Ca^{2+}, or other cytoplasmic factors responsible for the activation of a transport process (Adorante and Cala, 1987). For example, removal of Na from the apical bath results in an acidification of the RPE (Hughes et al., 1989). Thus cellular acidification may somehow inhibit RVI. However, when apical Na is removed in an HCO_3-free medium (a medium that also supports RVI), cell acidification is much less dramatic and slower in time course (Lin and Miller, 1989, and unpublished observations), yet RVI is completely inhibited. Because of the absence of Na/Ca exchange in the bullfrog RPE (Miller and Steinberg, 1977*b*), it is unlikely that a change in cell Ca^{2+} occurs after apical Na removal. In HCO_3-free medium changes in apical Cl or K have little or no effect on cell pH (Lin, H., and S. S. Miller, unpublished observations). Therefore, the K and Cl requirements for RVI are not mediated by changes in cell pH. Although it seems unlikely that changes in cell pH or Ca^{2+} are responsible for inhibition of RVI after ion substitution, inhibition of transport due to changes in some other cytoplasmic factor(s) cannot be ruled out. The observation that RVI is inhibited by bumetanide *and* requires Na, K, and Cl, we believe, strongly suggests that a Na,K,Cl cotransport mechanism mediates RVI in the bullfrog RPE.

The mechanism that underlies RVI is not understood. In other systems there is some evidence, albeit conflicting, that the phosphoinositide pathway may be involved (Cala, 1986; Grinstein et al., 1986).

Based on the thermodynamic calculations of Fig. 9, it seems likely that the mechanism responsible for RVI in the bullfrog RPE has a Na,K,Cl stoichiometry of 1:1:2. This conclusion has recently been corroborated in experiments using cultured human RPE cells (Kennedy, 1990). If one assumes that the bumetanide-inhibitable cotransporter has a Na,K,Cl stoichiometry of 1:2:3, as described for the squid axon (Russell, 1983), then its driving force in control Ringers (2 mM apical $[K^+]$) is $\sim +5{,}764$ J/mol. This large and outwardly directed driving force is not consistent with the observation that bumetanide inhibits net solute uptake (Edelman et al., 1988; Joseph and Miller, 1990; Miller and Edelman, 1990). Even when apical $[K^+]$ is isosmotically elevated to 5 mM, the calculated driving force for a 1Na, 2K, 3Cl cotransport mechanism is still outward ($\sim +1{,}253$ J/mol). Under these conditions, increasing the osmolality with mannitol will further increase the outward driving force, making it thermodynamically impossible for the cell to gain solute by this mechanism. Therefore, we can exclude the possibility that 1Na,2K,3Cl cotransport mediates RVI in the bullfrog RPE.

Anisosmotic and Isosmotic Changes in RPE Cell Volume

In the experiments of Figs. 3, *A* and *B*, 5, and 6, solution composition changes resulted in cell volume changes that were not associated with volume regulation. These volume changes are probably the result of a change in the forces driving steady-state net solute uptake and efflux mechanisms at the apical and basolateral membranes of the bullfrog RPE. For example, in the presence of 2 mM $[K^+]_o$ an increase in apical bath osmolality failed to initiate an RVI. Instead, the rapid osmometric phase was followed by a much slower secondary cell shrinkage that can be attributed to a net solute loss (Fig. 3, *A* and *B*). This secondary shrinkage is probably the result of a decrease in the net inward force driving electrogenic $NaHCO_3$ and electroneutral Na,K,2Cl cotransport and an increase in the force driving conductive K^+ and Cl^- efflux. This would tend to shrink the cells as solute efflux exceeds uptake. Because these effects on driving force increase with larger increases in media osmolality (as cell ion activities further increase), secondary cell shrinkage should be even larger at 280 mosmol than at 255 mosmol. The data shown in Fig. 3 support this notion.

Increasing apical K^+ from 2 to 5 mM isosmotically causes the cells to swell by ~7–10% in 10–15 min (see Methods and Fig. 5). This indicates that under these conditions net solute uptake exceeds net efflux. In this case the $NaHCO_3$ and Na,K,Cl cotransporters are also most likely the cause of RPE cell swelling. Here the K-induced depolarization of V_a stimulates apical electrogenic $NaHCO_3$ uptake, while solute uptake via electroneutral Na(K)Cl cotransport is directly stimulated by increasing apical $[K^+]$ (Edelman et al., 1988; Hughes et al., 1989; Miller and Edelman, 1990). Conductive K^+ flux out of the apical membrane will tend to be reduced when apical $[K^+]$ is raised, which will also favor cell swelling.

Removal of apical Na by isosmotic replacement with NMDG (Fig. 6) resulted in a cell shrinkage by ~15%. This observation is consistent with the reversal of the driving forces, now directed out of the cell, for $NaHCO_3$ and Na,K,Cl cotransport. As indicated in the Methods, a 10-fold reduction in apical HCO_3 (constant P_{CO_2}), from 27.5 to 2.75 mM, caused a ~15% cell shrinkage ($n = 4$ cells and 3 tissues). This decrease in cell volume supports our previous observation that apical HCO_3 reduction inhibits or reverses the $NaHCO_3$ cotransporter (Hughes et al., 1989).

Voltage Changes Associated with Changes in Cell Volume

Although the major focus of this work deals with the mechanism of cell volume regulation, the changes in V_a and V_b resulting from changes in cell volume require some discussion. The majority of the observed changes in V_a and V_n were small (<2 mV) and were probably the result of changes in the equilibrium potentials of conductive steady-state transport mechanisms following volume-induced cell ion activity changes. Furthermore, because the osmolality increases were made unilaterally (apical side only), sweeping away effects tending to increase ion activities in the basal unstirred layer and decrease ion activities in the apical unstirred layer (Diamond, 1979) may also contribute to changes in V_a and V_b.

After osmotic shrinkage with $[K^+]_o = 2$ mM, V_a and V_b depolarized transiently (see Fig. 3, *A* and *B*). These voltage changes were greater after hyperosmotic addition

of 50 mosmol mannitol than after addition of 25 mosmol. In these experiments volume regulation did not occur. These voltage changes are therefore not associated with RVI. On the other hand, increasing the apical bath osmolality in the absence of Na and the presence of 5 mM $[K^+]_o$ abolished the changes in V_a and V_b normally seen during cell shrinkage (Fig. 6). The mechanisms that mediate the membrane potential changes during osmotic cell shrinkage must therefore require apical Na.

There were, however, voltage changes observed during cell reswelling (volume regulation) that could result from activation of the Na,K,Cl cotransporter. Figs. 4 and 5 show that a small secondary depolarization of V_b (~1–2 mV) followed the time course of RVI. The depolarization of V_b, seen in most cells, is consistent with an increase in cell $[Cl]_i$ (mediated by an apical bumetanide-sensitive Na,K,Cl uptake mechanism), and the resulting decrease in E_{Cl} across the basal membrane Cl channel (Fong et al., 1988; Joseph and Miller, 1990).

Physiological Significance of RPE Cell Volume Regulation

RPE cell volume is kept constant, in the steady state, because some of the transport mechanisms that govern transepithelial flow also maintain the balance between net solute uptake and efflux. Alterations in net transport could be caused by light- or dark-induced changes in subretinal $[K^+]_o$. For example, in the present experiments we found that isosmotic elevation of apical $[K^+]$ from 2 to 5 mM caused the RPE cells to swell by ~7% and remain swollen. This $[K^+]_o$-induced swelling may serve a physiological function. For example, it has been shown that ouabain-induced cell swelling enhances retinal–RPE adhesivity (Marmor, 1989). Therefore, even small increases in RPE cell volume can have functional significance, in this case to enhance retina–pigment epithelial adhesion.

Another source of cell volume perturbation is suggested by the phagocytic relationship that exists between the RPE and the photoreceptor outer segments, which are renewed on a diurnal basis throughout the life of the organism. The steady-state growth of the outer segments is balanced by the equally voracious digestive capacity of the RPE cells. In the rat eye, for example, each RPE cell digests the equivalent of 7.5 photoreceptor outer segments per day, each one ~2 μm in diameter and 50 μm long (Bok, 1985). The rod photoreceptors undergo a burst of phagocytic activity at light onset (Basinger et al., 1976; La Vail, 1976), which, if osmotically significant, would require a mechanism for regulatory volume decrease (Adorante and Miller, 1990).

The subretinal space is bounded by three cell types: photoreceptors, RPE, and Muller cells. In principal, the volume of this extracellular space could be regulated by transport processes in all three cell types. Given their intimate anatomical and metabolic relationship, it would not be surprising if one or more of these cells delivered an osmotic load to the subretinal space during the light or dark. For example, the frog photoreceptors contain significant amounts of taurine (40–50 mM), some of which is released during the light (Orr et al., 1976; Salceda et al., 1977). In the dark, photoreceptor (and retinal) glycolysis is high and subretinal pH is relatively acidic (0.2 pH units), suggesting the accumulation of subretinal lactate (Winkler, 1983; Steinberg, 1987; Yamamoto and Steinberg, 1989). If these metabolites or others alter the osmolality of the subretinal space, changes in RPE cell

volume would be compensated for by the subsequent activation of volume regulatory transport mechanisms.

The recent report by Huang and Karwoski (1989) indicates that subretinal volume in the intact bullfrog eye increases or decreases by 5–10% after 70–90 s of illumination or dark, respectively. We have found that isosmotic changes of apical K^+, in the same range that occurs during light/dark transitions, produces similar changes in RPE cell volume (magnitude and time course). This comparison suggests that the RPE may play a major role in regulating subretinal volume in the intact eye.

It will be important to determine the exact relationship between the cotransporter-mediated changes in RPE cell volume, the overall physiology of the cell (e.g., phagocytosis and pH_i regulation), and the chemical composition of the subretinal space in the light and the dark.

This work was supported by National Institutes of Health grants EY-02205 and RCDA EY-00242 (to Dr. Miller) and core grant EY-02176 and National Research Service Award EY-05968 to Dr. Adorante.

Original version received 15 January 1990 and accepted version received 14 June 1990.

REFERENCES

Adorante, J. S., and P. M. Cala. 1987. Activation of electroneutral K flux in *Amphiuma* red blood cells by *N*-ethylmaleimide. Distinction between K/H exchange and KCl cotransport. *The Journal of General Physiology.* 90:209–227.

Adorante, J. S., and S. S. Miller. 1989. Na,K,Cl cotransport regulates frog retinal pigment epithelial (RPE) cell volume. *Investigative Ophthalmology and Visual Science.* 30(Suppl.):169. (Abstr.)

Adorante, J. S., and S. S. Miller. 1990. Regulatory volume decrease in frog retinal pigment epithelium. *Investigative Ophthalmology and Visual Science.* 31(Suppl.):343 (Abstr.)

Basinger, S., R. Hoffman, and M. Matthes. 1976. Photoreceptor shedding is initiated by light in the frog retina. *Science* 194:1074–1076.

Besharse, J. C., P. M. Iuvone, and M. E. Pierce. 1987. Regulation of rhythmic photoreceptor metabolism: a role for post-receptoral neurons. *Progress in Retinal Research.* 7:1–41.

Bird, A. C. 1989. Pathogenesis of serious detachment of the retina and pigment epithelium. *In* The Retina. Vol. 2. S. J. Ryan, editor. C. V. Mosby Company, St. Louis. 99–105.

Bok, D. 1985. Retinal photo receptor-pigment epithelium interactions: Friedenwald Lecture. *Investigative Ophthalmology and Visual Science.* 26:1659–1694.

Cala, P. M. 1980. Volume regulation by *Amphiuma* red blood cells. The membrane potential and its implications regarding the nature of the ion-flux pathways. *Journal of General Physiology.* 69:683–708.

Cala, P. M. 1983. Volume regulation by red blood cell: mechanisms of ion transport. *Molecular Physiology.* 4:35–52.

Cala, P. M. 1986. Volume-sensitive alkali metal-H transport in *Amphiuma* red blood cells. *Current Topics in Membrane and Transport.* 26:79–99.

Coles, J. A., and M. Tsacopoulos. 1977. A making of fine doubled-barrelled potassium-sensitive micro-electrodes for intracellular recording. *The Journal of Physiology.* 270:12p–14p.

Cotton, C. U., A. M. Weinstein, and L. Reuss. 1989. Osmotic water permeability of *Necturus* gallbladder epithelium. *The Journal of General Physiology.* 93:649–679.

Diamond, J. M. 1979. Osmotic water flow in leaky epithelia. *Journal of Membrane Biology.* 51:195–216.

Edelman, J. L., S. S. Miller, and B. A. Hughes. 1988. Regulation of chloride transport by frog retinal pigment epithelium. *FASEB Journal.* 2:A1722. (Abstr.)

Eveloff, J., and D. G. Warnock. 1987. Activation of ion transport systems during cell volume regulation. *American Journal of Physiology.* 252 (*Renal Fluid and Electrolyte Physiology* 21): F1–F10.

Fong, C. Y., S. Bialek, B. A. Hughes, and S. S. Miller. 1988. Modulation of intracellular Cl in bullfrog frog retinal pigment epithelium (RPE). *Federation of American Societies for Experimental Biology* (*FASB*). 2:1722. (Abstr.)

Geck, P., C. Pietrzyk, B. C. Burkhardt, B. Pfeiffer, and E. Heinz. 1980. Electrically silent cotransport of Na, K and Cl in Erlich cells. *Biochemica et Biophysica Acta.* 600:432–447.

Grinstein, S., J. D. Goetz-Smith, D. Steward, B. J. Beresford, and A. Mellors. 1986. Protein phosphorylation during activation of Na/H exchange by phorbol esters and osmotic shrinkage. *Journal of Biological Chemistry.* 261:8009–8016.

Haas, M. 1989. Properties and diversity of Na-K-Cl cotransporters. *Annual Review of Physiology.* 51:443–457.

Haas, M., W. F. Schmidt III, and T. J. McManus. 1982. Catecholamine-stimulated ion transport in duck red cells. Gradient effects in electrically neutral [Na + K + 2Cl] cotransport. *Journal of General Physiology.* 80:125–147.

Hoffman, E. K., and L. O. Simonsen. 1989. Membrane mechanisms in volume and pH regulation in vertebrate cells. *Physiological Reviews.* 69:315–389.

House, C. R. 1976. Water and Transport in Cells and Tissues. Edward Arnold Publishers, Ltd., London. 192–196.

Huang, B., and C. Karwoski. 1989. Changes in extracellular space in the frog retina. *Investigative Ophthalmology and Visual Science.* 30(Suppl.):64. (Abstr.)

Hughes, B. A., J. S. Adorante, S. S. Miller, and H. Lin. 1989. Apical $NaHCO_3$ cotransport. A mechanism for HCO_3 absorption across the retinal pigment epithelium. *Journal of General Physiology.* 94:125–150.

Hughes, B. A., S. S. Miller, and D. Farber. 1987. Adenylate cyclase stimulation alters transport in frog retinal pigment epithelium. *American Journal of Physiology.* 252 (*Cell Physiology*): C385–C395.

Hughes, B. A., S. S. Miller, D. P. Joseph, and J. L. Edelman. 1988. cAMP stimulates the Na^+-K^+ pump in frog retinal pigment epithelium. *American Journal of Physiology.* 254 (*Cell Physiology*): C84–C98.

Hughes, B. A., S. S. Miller, and T. E. Machen. 1984. Effects of cyclic AMP on fluid absorption and ion transport across frog retinal pigment epithelium. *The Journal of General Physiology.* 83:875–899.

Joseph, D., and S. S. Miller. 1990. Apical and basal membrane ion transport mechanisms in the bovine retinal pigment epithelium. *Journal of Physiology.* In press.

Kennedy, B. G. 1990. Na^+-K^+-Cl^- cotransport in cultured cells derived from human retinal pigment epithelium. *American Journal of Physiology.* 259 (*Cell Physiology*): C29–C34.

Kregenow, F. M. 1971. The response of duck erythrocytes to hypertonic media. Evidence for a volume controlling mechanism. *Journal of General Physiology.* 58:396–412.

La Cour, M. 1989. Rheogenic sodium bicarbonate co-transport across the retinal membrane of the frog retinal pigment epithelium. *Journal of Physiology.* 419:539–553.

Larson, M., and K. R. Spring. 1987. Volume regulation in epithelia. *Current Topics in Membranes and Transport.* 30:105–123.

La Vail, M. M. 1976. Rod outer and segment disk shedding in rat retina: relationship to cyclic lighting. *Science.* 194:1071–1074.

Lin, H., and S. S. Miller. 1989. $[K^+]_o$-induced changes in apical membrane voltage (V_a) modulate pH_i in frog retinal pigment epithelium. *Investigative Ophthalmology and Visual Science* 30(Suppl.): 168. (Abstr.)

Lohr, J. W., and J. J. Grantham. 1986. Isovolumetric regulation of isolated S_2 proximal tubules in anisotonic media. *Journal of Clinical Investigation.* 78:1165–1172.

Marmor, M. E. 1989. Mechanisms of normal retinal adhesion. *In* The Retina. Vol. 3. S. J. Ryan, editor. C. V. Mosby Company, St. Louis. 71–87.

Miller, S. S., and J. L. Edelman. 1990. Active ion transport pathways in the bovine retinal pigment epithelium. *Journal of Physiology.* 424:283–300.

Miller, S. S., and D. Farber. 1984. Cyclic AMP modulation of ion transport across the frog retinal pigment epithelium. *The Journal of General Physiology.* 83:853–874.

Miller, S. S., and R. S. Steinberg. 1977*a*. Passive properties of frog retinal pigment epithelium. *Journal of Membrane Biology.* 36:337–372.

Miller, S. S., and R. S. Steinberg. 1977*b*. Active transport of ions across the frog retinal pigment epithelium. *Experimental Eye Research.* 25:235–248.

Miller, S. S., R. S. Steinberg, and B. Oakley. 1978. The electrogenic sodium pump of the frog retinal pigment epithelium. *Journal of Membrane Biology.* 44:259–279.

Neher, E., and H. D. Lux. 1973. Rapid changes of potassium concentration at the outer surface of exposed single neurons during membrane current flow. *The Journal of General Physiology.* 61:385–399.

O'Grady, S. M., H. C. Palfrey, and M. Field. 1987. Characteristics and functions of Na-K-Cl cotransport in epithelial tissues. *American Journal of Physiology.* 253 (*Cell Physiology* 22): C177–C192.

Orr, H. T., A. I. Cohen, and O. H. Lowry. 1976. The distribution of taurine in the vertebrate retina. *Journal of Neurochemistry.* 26:609–611.

Pederson, J. E. 1989. Fluid physiology of the subretinal space. *In* The Retina. Vol. 3. S. J. Ryan, editor. C. V. Mosby Company, St. Louis. 89–102.

Reuss, L. 1985. Changes in cell volume measured with an electro-physiologic technique. *Proceedings of the National Academy of Sciences USA.* 83:6014–6018.

Russell, J. M. 1983. Cation coupled chloride influx in the squid axon. Role of potassium and stoichiometry of the process. *Journal of General Physiology.* 81:909–925.

Salceda, R., A. M. Lopez-Colome, and H. Pasantes-Morales. 1977. Light-stimulated release of ^{35}S-taurine from frog retinal outer segments. *Brain Research.* 135:186–191.

Steinberg, R. H. 1987. Monitoring communications between photoreceptors and pigment epithelial cells: effects of "mild" systemic hypoxia. *Investigative Ophthalmology and Visual Sciences.* 28:1888–1904.

Steinberg, R. H. 1988. Electrical interactions between the RPE and the photoreceptors. *In* International Symposium on the Retina. M. Tso, editor. J. B. Lippencott, Philadelphia. 60–79.

Steinberg, R. H., R. A. Linsenmeier, and E. R. Griff. 1985. Retinal pigment epithelial contributions to the electroretinogram. *In* Progress in Retinal Research. Vol. IV. N. Osborne and G. Chader, editors. Pergamon Press Inc., Elmsford, NY. 33–66.

Winkler, B. 1983. The intermediary metabolism of the retina: biochemical and functional aspects. *In* Biochemistry of the Eye. R. E. Anderson, editor. American Academy of Ophthalmology, San Francosco. 227–247.

Yamamoto, R., and R. H. Steinberg. 1989. Effects of mild systemic hypoxia on $[K^+]_o$ outside rod photoreceptors in cat. *Society for Neuroscience.* 15:206. (Abstr.)